Supporting Information

Scaled Conductance Quantization Unravels Switching Mechanism in Organic Ternary Resistive Memories

Xue-Feng Cheng,[a] Yao Zhao,[b] Wen Ye,[a] Chuang Yu,[a] Jing-Hui He,[a] Fu-Yi Wang[b] and Jian-Mei Lu[a]**

Experimental Section

Materials: Squaric acid, 4-butylaniline, n-butanol, toluene, chloroform and hexane were purchased from TCI or Adamas and used without further purification.
Synthesis of 2-((4-butylphenyl)amino)-4-((4-butylphenyl)iminio)-3-oxocyclobut-1-en-1-olate (**SA-Bu**): First, 1.1406 g squaric acid (10 mmol) and 2.9846 g 4-butylaniline (20 mmol) were dissolved in 40 mL mixed solvent (n-butanol/toluene with equal amount in volume). The mixture was stirred and refluxed for 12 h. The final mixture was filtrated and washed with chloroform and hexane three times. A yellow powder was obtained as molecular SA-Bu. ^{1}H NMR (400 MHz, DMSO-d_6) δ 10.04 (s, 1H), 7.46 (d, J = 7.9 Hz, 4H), 7.24 (d, J = 8.0 Hz, 4H), 2.61 (d, J = 7.7 Hz, 4H), 1.62 – 1.56 (m, 4H), 1.36 (d, J = 7.4 Hz, 4H), 0.95 (t, J = 7.3 Hz, 6H).

Memory device fabrication: The indium tin oxide (ITO) glass was cleaned by detergent and was subsequently washed with deionized water, acetone and ethanol, and each step was performed with ultrasonication for a duration of 10 min. Dried ITO substrates were treated with oxygen plasma for 10 min. After that, SA-Bu was thermally evaporated onto the ITO substrate under a 10^{-6} Torr vacuum. Next, a shadow mask was pasted to cover the organic film, and the Al electrode was evaporated with a thickness of 100 nm (or a 100 nm Au electrode was deposited through the magnetron sputtering method).

Surface modification of ITO substrates: Initially, 15.8 mg (10 mmol) phenylphosphonic acid (PPA) and 19.4 mg (10 mmol) octylphosphonic acid (OPA) were dissolved in 100 mL ethanol. Then, clean ITO substrates were immersed into a prepared solution, and the solvent was left evaporate in atmospheric conditions at room temperature. Once the volume fell below the substrate, the ITO substrates were cleaned in ethanol by sonication to remove the phosphonic acid residue. Then, the ITO substrates were dried under a vacuum at 60 °C. The dried ITO substrates were sonicated again for 30 min in a trimethylamine/ethanol solution (1:20 volume ratio), which was followed by washing in absolute ethanol.

Measurements and general methods: NMR spectrum of SA-Bu was obtained from Inova 400 MHz FT-NMR spectrometer. X-ray diffraction patterns were obtained from Shimadzu XRD-6000 spectrometer with a $Cu_{K\alpha}$ monochromatic radiation source at 40 kV and 30 mA. MFP-3DTM (Digital Instrument/Asylum Research) AFM instrument was applied to characterize the surface morphology and conductivity of the fabricated film devices. The current-voltage (I-V) and current-time (I-t) characteristics of the memory devices were measured by Keithley 4200-SCS. SEM images were taken by using a Hitachi S-4700 scanning electron microscope. Thermo Fisher Escalab X-Ray

photoelectron spectrometer operated the argon ion etching and obtained XPS spectra. ToF-SIMS analysis and depth profiling were conducted using a ToF-SIMS V spectrometer (IONTOF GmbH, Munster, Germany). Dual-beam experiments were performed using a 20 keV argon cluster ion beam (Ar^{n+}) as sputtering beam and a 30.0 keV Bi^{3+} beam as analysis beam. High mass resolution spectra were collected in the positive ion mode over a 150 × 150 μm^2 area upon a pulsed analysis Bi^{3+} beam at the center of a 400 × 400 μm^2 crater eroded by Ar^{n+} sputtering source. Charge compensation was always applied during the experiments to prevent charge accumulation.

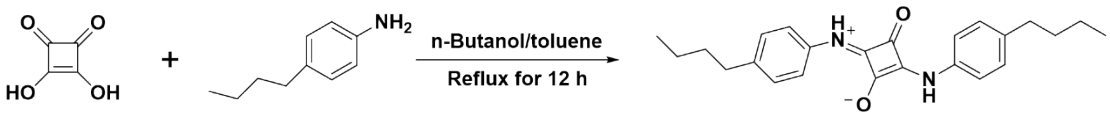

Scheme S1. Synthesis route of molecule SA-Bu.

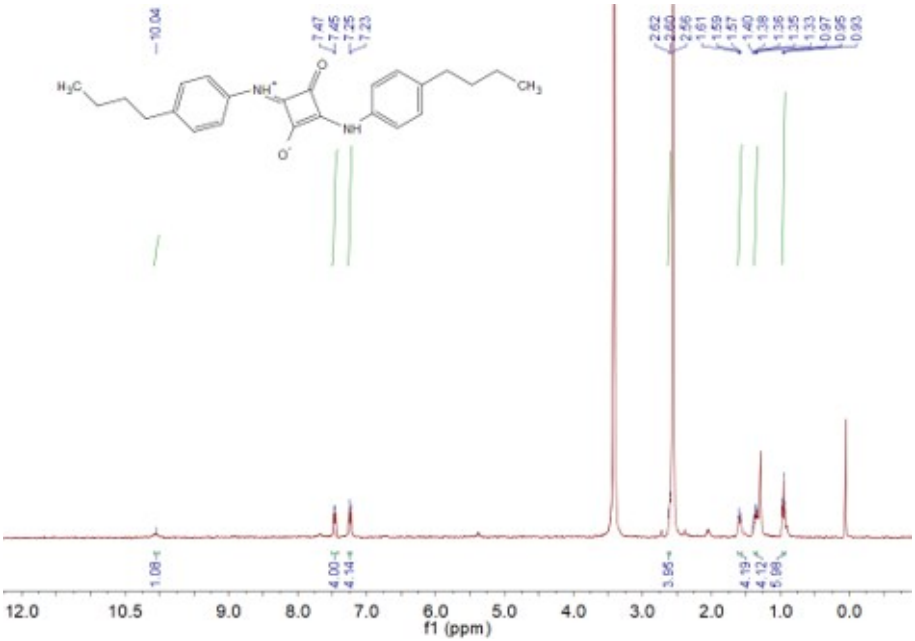

Figure S1. ^1H NMR spectrum of SA-Bu molecule in d_6-DMSO.

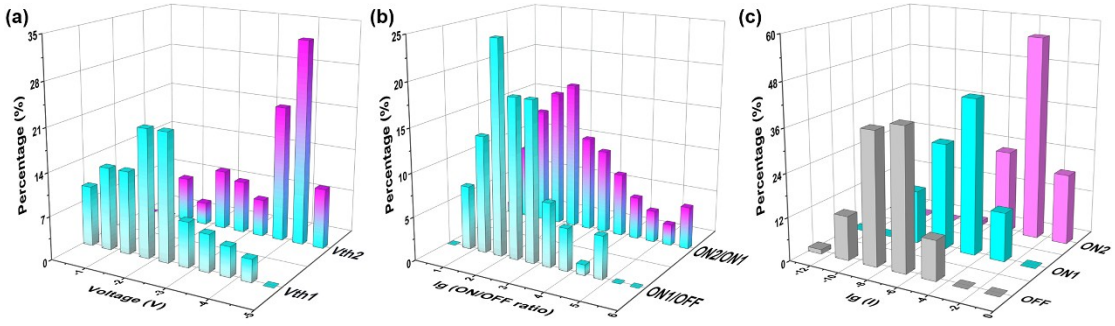

Figure S2. The distribution of (a) threshold voltages, (b) ON/OFF ratio and (c) different current levels. The distribution data collected from the ternary memories in 200 samples.

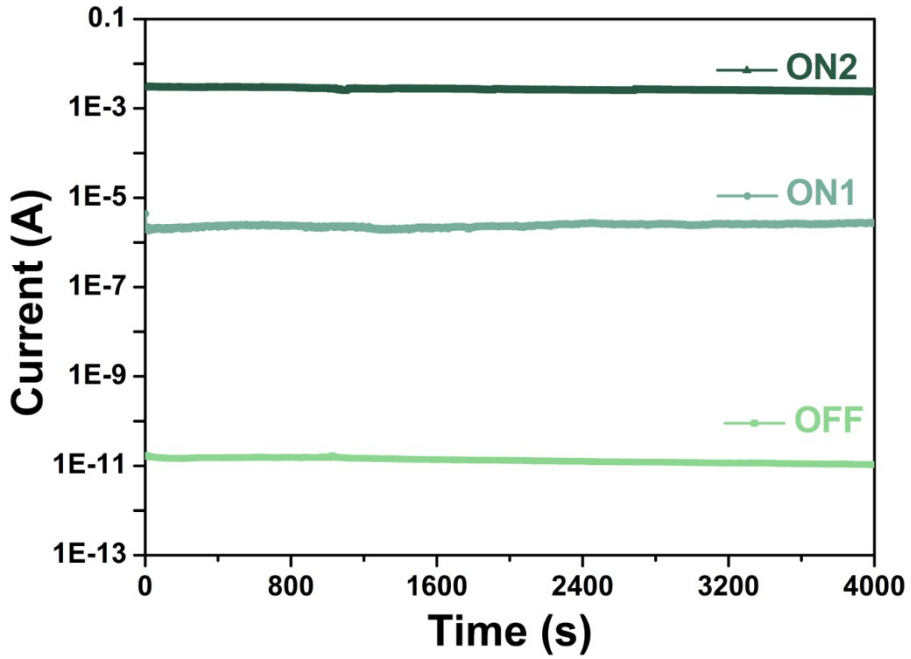

Figure S3. Characteristic retention stability of ITO/SA-Bu/Al device under continuous -1 V stress.

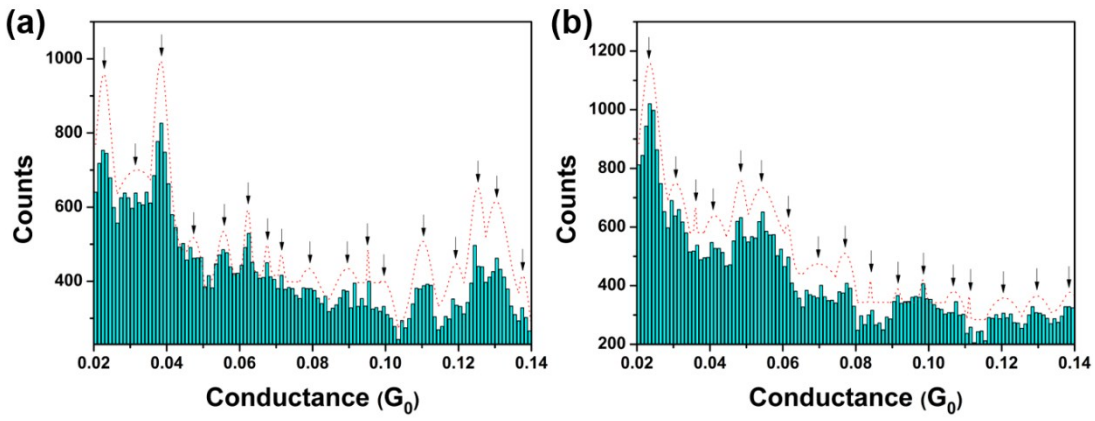

Figure S4. Counts-Conductance plot of ITO/SA-Bu/Al devices on a sample size of 1000: (a) 87 nm SA-Bu and (b) 108 nm SA-Bu.

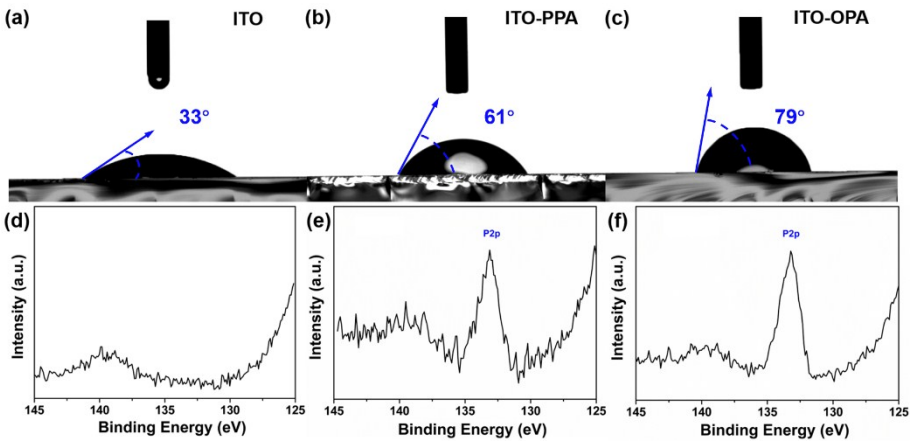

Figure S5. Wettability tested in air and XPS spectra (P2p) of (a, d) ITO substrate without modification, modified with (b, e) PPA and (c, f) OPA.

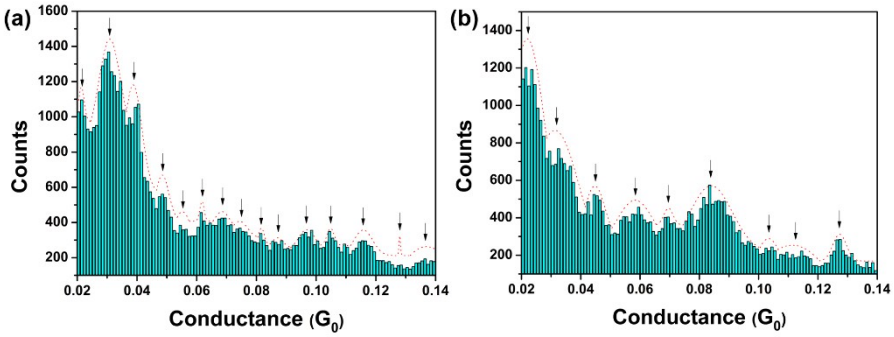

Figure S6. Counts-Conductance plot of Al/SA-Bu/ITO devices modified by (a) PPA and (b) OPA based on one thousand writing procedure.

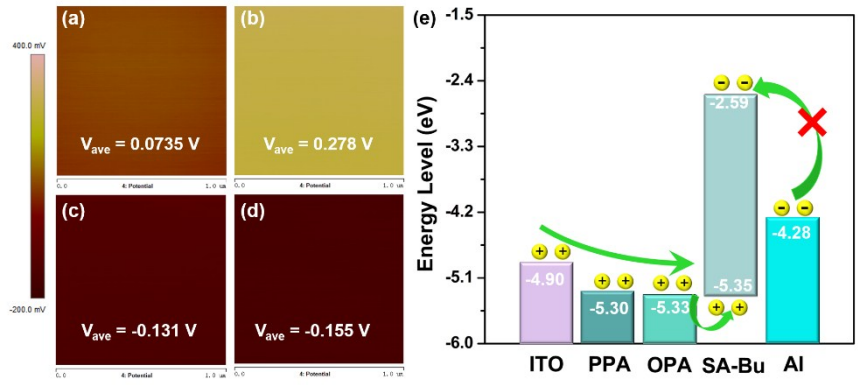

Figure S7. KPFM test of (a) Fresh Au surface; (b) original ITO surface; (c) PPA modified ITO surface; (d) OPA modified ITO surface, V_{ave} is the average potential of 1 μm*1 μm area. (e) Energy diagrams of ITO/SA-Bu/Al device with/without surface modification.

The work functions of ITO, ITO-PPA and ITO-OPA were determined from relative surface potentials

via Kelvin probe mode. During the testing process, voltage was applied on the tips. The obtained V_{CPD} is the electrical potential differences of tips and samples. It obeys equation (S1):

$$V_{CPD} = V_{Tip} - V_{sample} \quad \text{(S1)}$$

Fresh Au film was used to calibrate the potential of tip. According to **Figure S6a-d**, the work functions of ITO, ITO-PPA and ITO-OPA were obtained as -4.90 eV, -5.30 eV and -5.33 eV respectively. The energy levels of HOMO and LUMO obtained from UV-vis spectrum and cyclic voltammogram as previously reported. [S1] The energy levels of each component were list in **Figure S6e**. The injection barriers for holes are much smaller than that for electrons, indicating the holes dominate the transportation of charge carriers in devices. After modifying by PPA and OPA, the hole injection barriers reduced from 0.45 eV to 0.05 eV and 0.03 eV. Therefore, surface modification of ITO substrates with PPA and OPA effectively reduced the energy consumed to overcome the barriers.

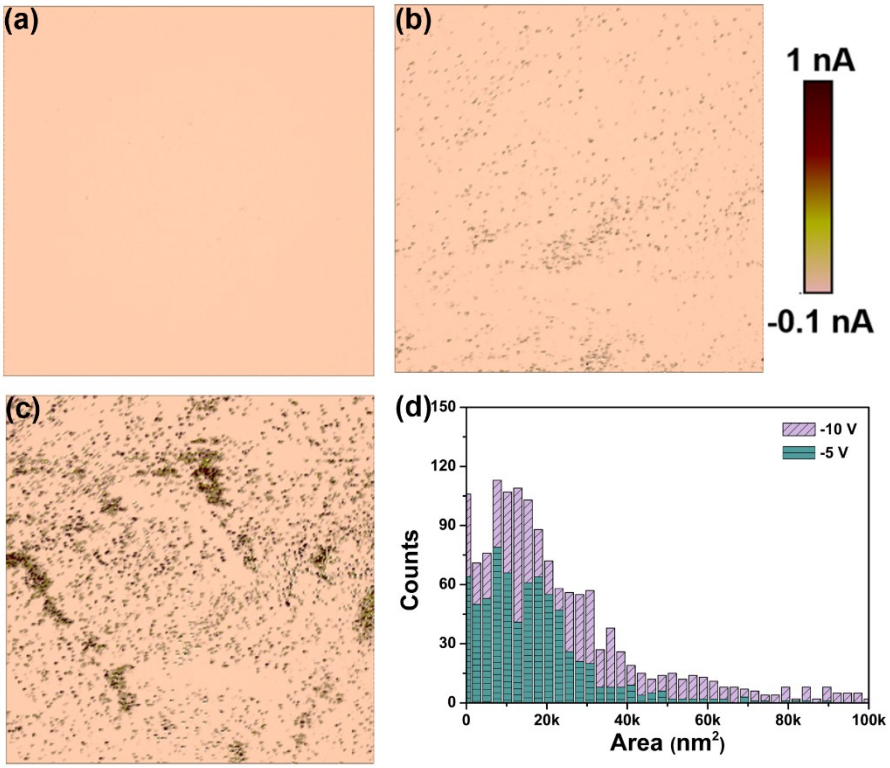

Figure S8. Top-view of c-AFM images of memory device under (a) 0 V, (b) -5 V and (c) -10 V. (d) Distribution of conductive channels' area.

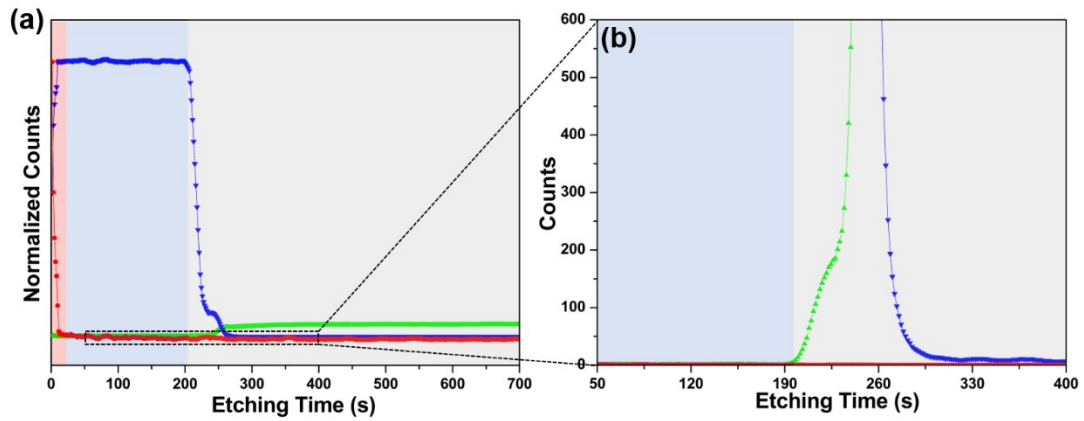

Figure S9. ToF-SIMS analysis and depth profiling on SA-Bu/ITO glass device.

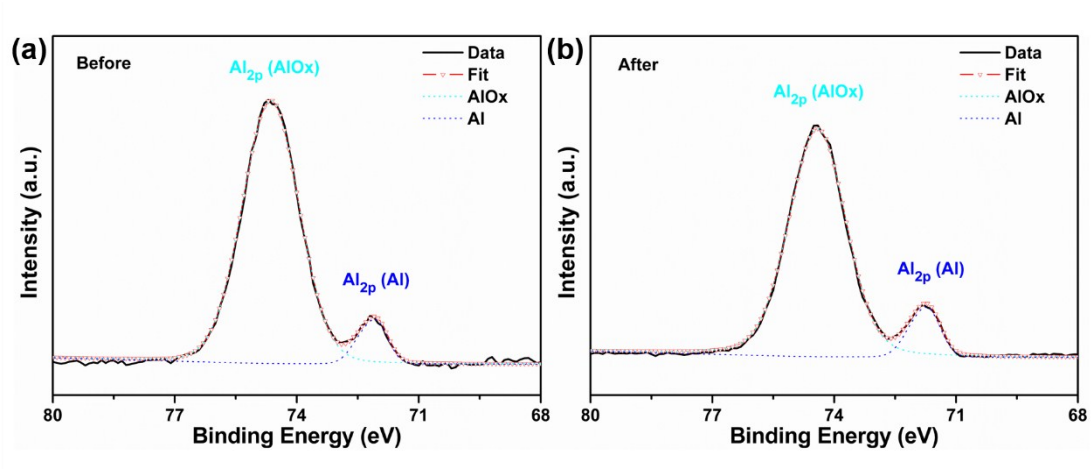

Figure S10. XPS patterns of ITO/SA-Bu/Al device (a) before and (b) after voltage sweep.

Table S1. The contents of aluminum in metal and metal oxide states.

	XPS		
	Al:AlOx (%)[a]	**Al (Atom%)**	**O (Atom%)**
Before	8.75	32.77	67.23
After	11.30	35.16	64.84

a. The integrated area of Al 2p in metal aluminum state/the integrated area in aluminum oxide state obtained from XPS patterns.

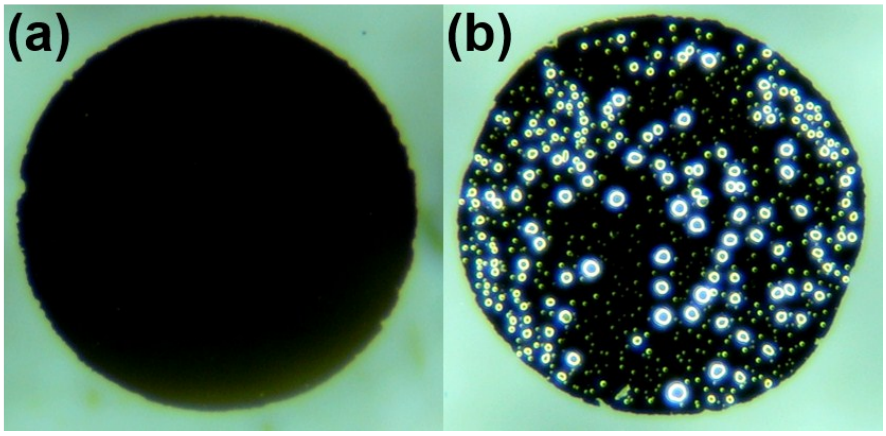

Figure S11. Photographs of (a) original Al electrode and (b) Al electrode of ITO/Al device after voltage sweep.

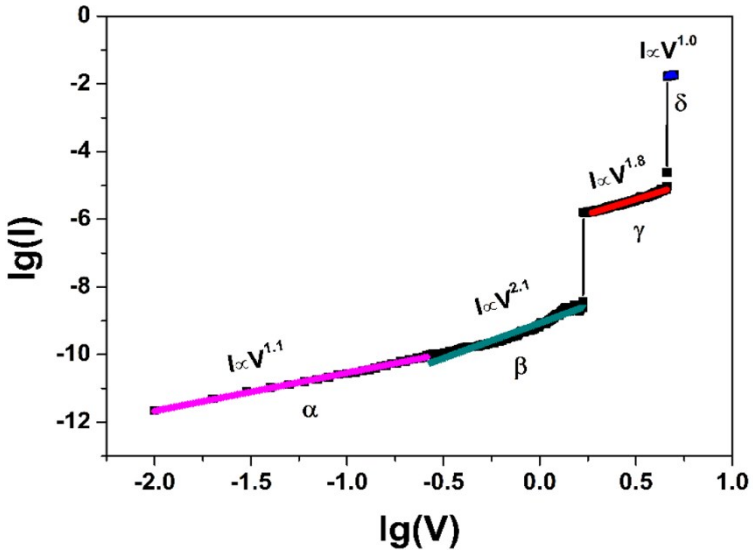

Figure S12. Current–voltage (I–V) relationship in log–log plot.

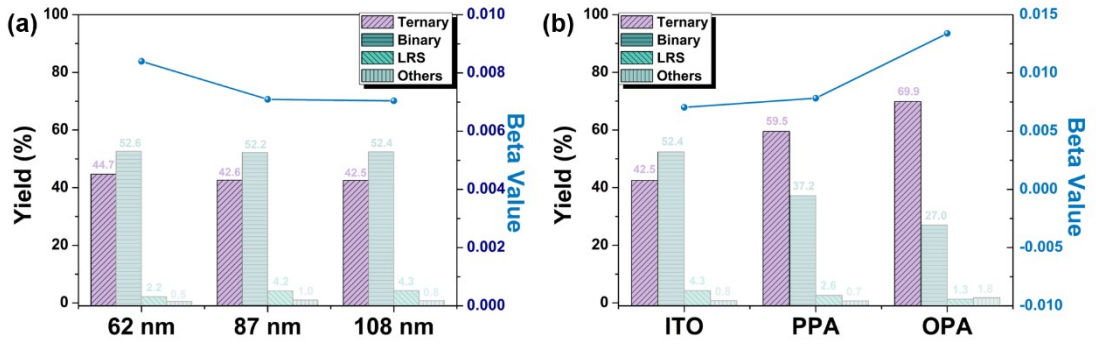

Figure S13. (a) Histogram of memory performance based on ITO/SA-Bu/Al with different thicknesses and corresponding *β* values. (b) Histogram of memory performance based on memory devices with/without surface modification and corresponding *β* values.

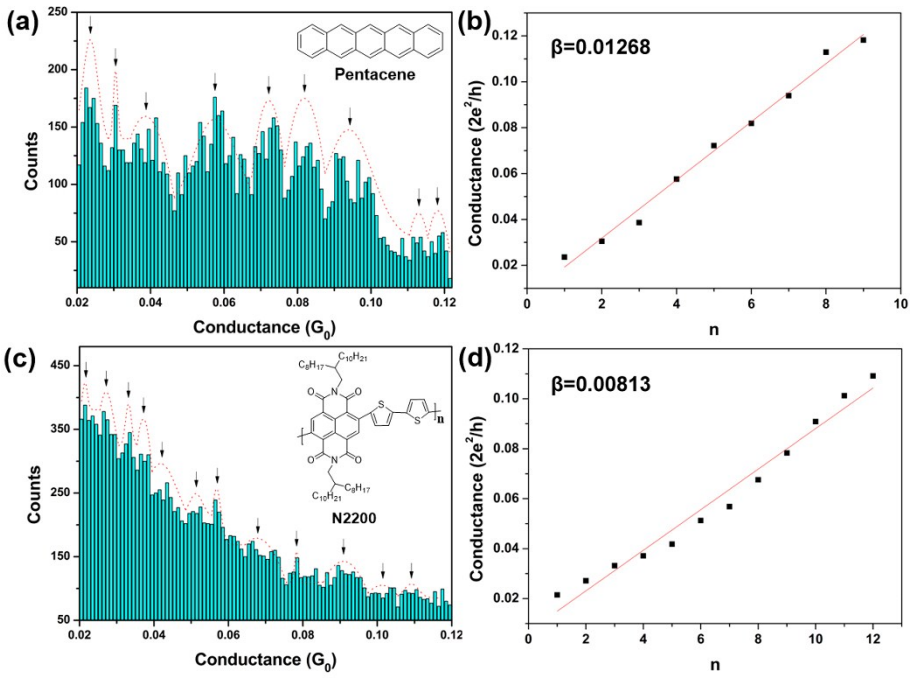

Figure S14. Counts-Conductance plot of (a) Al/Pentacene/ITO devices and (c) Al/N2200/ITO based on two hundred writing procedure. (b, d) Corresponding linear fitting of the peak positions.

References:

S1. X. Hou, X. Xiao, Q.-H. Zhou, X.-F. Cheng, J.-H. He, Q.-F. Xu, H. Li, N.-J. Li, D.-Y. Chen and J.-M. Lu, *Chem. Sci.*, 2017, **8**, 2344-2351.